Calibrating AIS Images Using the Surface as a Reference

M. O. Smith, D. A. Roberts, H. M. Shipman, J. B. Adams, S. C. Willis and A. R. Gillespie
University of Washington
Seattle, WA. 98195

ABSTRACT

We have tested a method of evaluating the initial assumptions and uncertainties of the physical connection between AIS image data and laboratory / field spectrometer data. To first order, the Tuscon AIS-2 image (flight #601) connects to laboratory reference spectra by an alignment to the image spectral endmembers through a system gain and offset for each band.

We have chosen to calibrate images to reflectance so as to transform the image into a measure that is independent of the solar radiant flux. This transformation also makes the image spectra directly comparable to data from laboratory and field spectrometers. Our objective in this paper is to test a method for calibrating AIS images using the surface as a reference. The surface heterogeneity is defined by laboratory / field spectral measurements.

We have developed an approach to calibration that maps the n-dimensional volume defined by image spectra into the n-dimensional volume defined by laboratory/ field reference spectra. The dimension of the volume is equivalent to the number of image bandpasses. We assume that to first order 1) the image spectra are linear mixtures of the laboratory or field reference spectra and 2) that there is a set of system gains and offsets for each band. However, it is not necessary that the image spectra be mixtures of the reference spectra; they could be pure endmembers themselves. The system gains and offsets include all contributions from the entire system (e.g., atmosphere, solar spectrum, instrument, lighting geometry, etc.) not solely those due to the instrument.

We tested these assumptions on an AIS-2 image (flight #601) obtained in September 1986 of the Tucson Mountains just west of Tucson, Arizonia. The instrument was flown in rock mode and included the wavelength range from 1200 nm to 2500 nm. We used only bandpasses where the signal to noise ratio was near 100 or better, which resulted in a reduction of the original 128 bands (rock mode) to 64 bands. Prior to analysis the image was destriped by adjusting gains for each column to equalize the column means.

Representative spectra of surface samples were measured on a Beckman DK-2A spectrometer. We term this set of spectra the reference endmembers, since they describe pure surface components (Figure 1). Other reference spectra could be modeled as linear mixtures of these spectra. In addition to these three spectra the reference endmembers also include the spectrum shade which has 0% reflectance. A precise definition of the endmember shade is given in Adams et al. 1986. These reference spectra are used to define the n-dimensional volume of all reference spectral measurements.

To complement the reference endmembers, we need to determine a set of image endmembers such that they define the n-dimensional volume of the image. The image volume is defined by single pixel image endmembers that, when linearly mixed,

adequately fit the image spectral variance and yield fractions between 0 and 1. The spectral image endmembers do not necessarily have any physical identity. For the 64 selected AIS-2 bands we found the linear mixtures of four image endmember spectra could model the fans south of the Desert Museum (Figure 2) to within 10 DN rms error. The rms error is computed as the difference between the measured image data and that predicted by a least square fit of mixtures of the four endmembers. Only random spatial patterns were present in the rms error image indicating the four image endmembers adaquately defined the image n-dimensional volume.

The connection between the image endmembers and laboratory reference endmembers is made using the following equation:

$$G_b \, DN_{iem,b} + O_b = \Sigma \, F_{em} \, R_{e,b} \tag{1}$$

subject to the constraint : $\Sigma \, F_{em} = 1$

where $DN_{iem,b}$ is the digital number for each image endmember for each band, G_b the system gain to convert image digital numbers to total hemispherical reflectance for each band b, O_b the offset in reflectance for each band b, F_{em} the fractional contribution of each reference spectral endmember, and $R_{e,b}$ the total hemispherical reflectance for each reference spectral endmember for each band b. The summation in Equation 1 is over the number of relevant spectral endmembers. The equation is solved iteratively first for the gains and offsets and then for the fractions F_{em}.

Equation 1 formalizes our hypothesis that the primary connection between the imaged surface and laboratory reference spectra involves first an alignment of mixed pixels in the image to unmixed reference spectra, and secondly a calibration between image digital numbers and total hemispherical reflectance. The calibration model uses a simple linear equation consisting of a single gain and offset for each band. However, imbedded in the gains and offsets are more than the instrument calibration; in addition, there are effects caused by the solar spectrum, the atmosphere, and differences in lighting geometry between image and laboratory measurement systems. We are testing whether or not the entire system including the atmosphere, solar spectrum, and conversion of bidirectional to total hemispherical reflectance can, to first order, be approximated by a linear equation.

The solution consists of finding the fractions F_{em} that align the mixed pixel endmember spectra from the image to the unmixed reference endmembers. The results of the alignment (Table 1) are physically realizable, i.e., the image endmember set consists of fractions between 0 and 1 for each reference endmember spectrum, and each image endmember spectrum fits well to linear combinations of the reference spectra (rms errors are all < 0.3% reflectance). Table 1 now makes possible a physical identification of the image endmembers from the reference spectra. For example, em-1 is predominantly equivalent to an arkose spectrum (f=0.6 arkose), but unlike the reference spectrum of arkose, is mixed with vegetation, shade, and rhyolite. Similarly, each of the other image endmembers connect predominantly to an equivalent reference endmember spectrum.
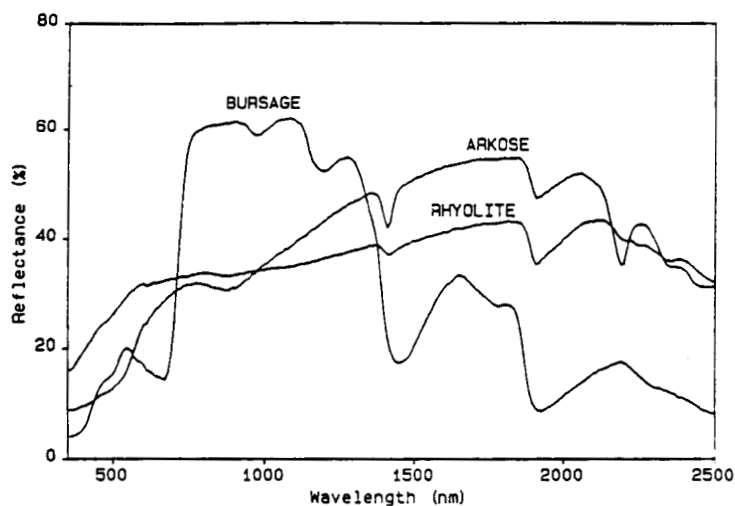
Figure 1. Total hemispherical reflectance of the field spectral endmembers. Measurements were made with a Beckman 2K-DA spectrometer.
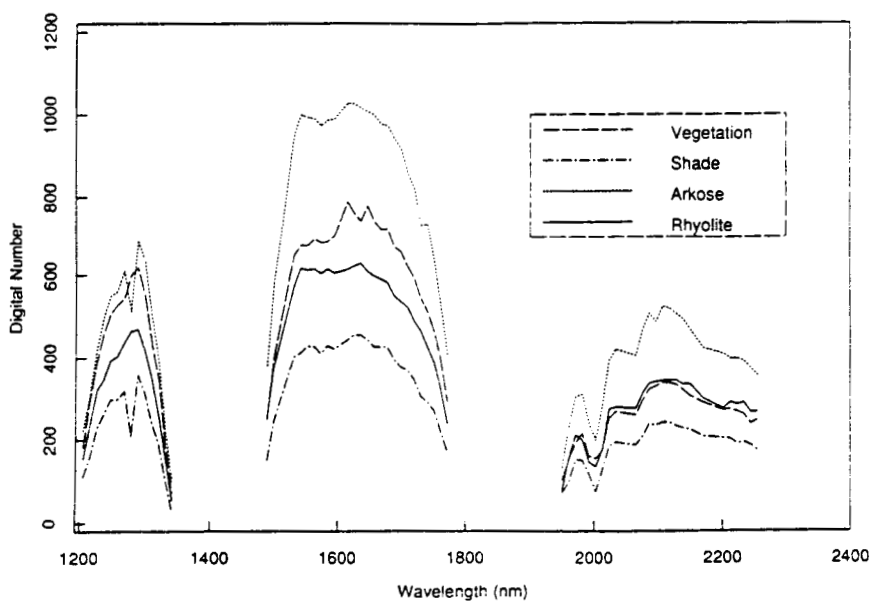

Figure 2. Raw digital numbers of the image spectral endmembers. Wavelengths shown were those with high signal to noise ratios used in our analysis. Note abscissas for Figures 1 and 2 are different.

Table I. Results of Image Endmember Alignment to Reference Spectra

| Image Endmember | Fraction of Reference Endmember | | | | |
	arkose	rhyolite	bursage	shade	rms error
em-1	0.60	0.14	0.24	0.03	0.002
em-2	0.01	0.52	0.21	0.27	0.001
em-3	0.36	0.02	0.42	0.19	0.002
em-4	0.03	0.32	0.14	0.51	0.002

The gains and offsets from Equation 1 characterize the total system response to a linear calibration. The predominant pattern in the gain curves (Figure 3) is an inverted response to the water bands at 1400 and 1900 nm. In addition, the CO_2 absorption bands near 2000 nm are evident. These characteristics are resolved in the gains because they are constant for the entire image. Similarly, the offsets for most bands (Figure 4) typically were below 1% reflectance. However, many bands near 1200 nm have erratic scatter and high offsets. This type of pattern is indicative of faulty detector elements in the two-dimensional CCD array of the AIS-2 instrument.

To test the appropriateness of the reference endmembers with respect to the image endmembers, we determined the quality of fit (correlation) between each of the four image and reference endmembers for each band independently (Figure 5). The wavelengths between 1200 nm and 1300 nm exhibit some of the variability observed in the offsets (Figure 5) and gains (Figure 3). This does not fit the pattern of variation we observe in the reference endmembers (Figure 1). We interpret the almost random variation in corrlelations between 1200nm and 1300nm, and the significantly lower correlations at 1900 nm to be typical of that caused by the instrumentation.

In contrast, the systematic lack of fit near 2200 nm corresponds to the absorption feature of the arkose reference spectra (Figure 1). A plot of the image and reference endmembers for the 2200 nm wavelength (Figure 6) illustrates the deviation of the arkose from a linear calibration. We interpret this lack of fit at 2200 nm as a mismatch between the image and reference arkose endmember spectrum. What we have interpreted as an arkose for the image endmember has the general shape of the reference arkose spectrum, but lacks the 2200 nm absorption band. Even though the arkose reference spectrum does not fit the image data at 2200 nm we can use the other three reference endmembers to determine the gains and offsets in this wavelength region to maintain calibration integrity.

To determine if areas in the image contained the 2200 nm clay absorption band found in the arkose reference spectrum, we examined the difference images between that predicted by mixtures of the calibrated image endmembers and the raw image. Three of the difference images corresponding to the bands of the 2200 nm clay absorption contained distinct spatial patterns relating to the reference arkose spectrum. Distinct spatial patterns in the difference images provide a means of determining if subtle absorption features present in the surface mineralogy can be detected over that of the AIS-2 instrument noise. Further resolution of the 2200 nm
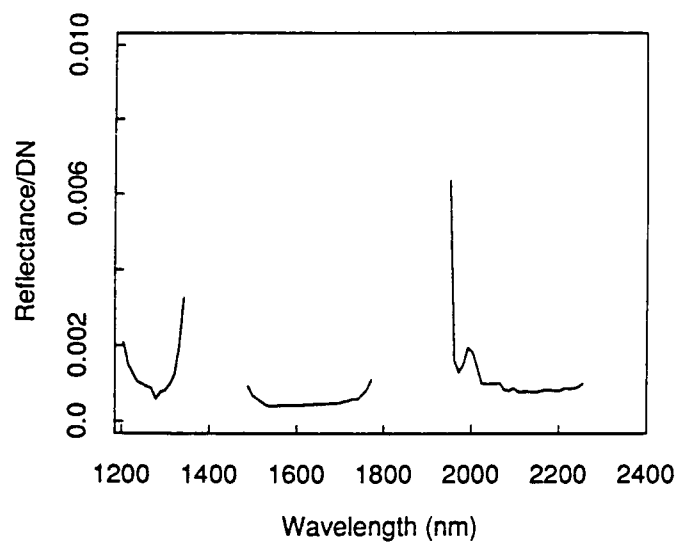
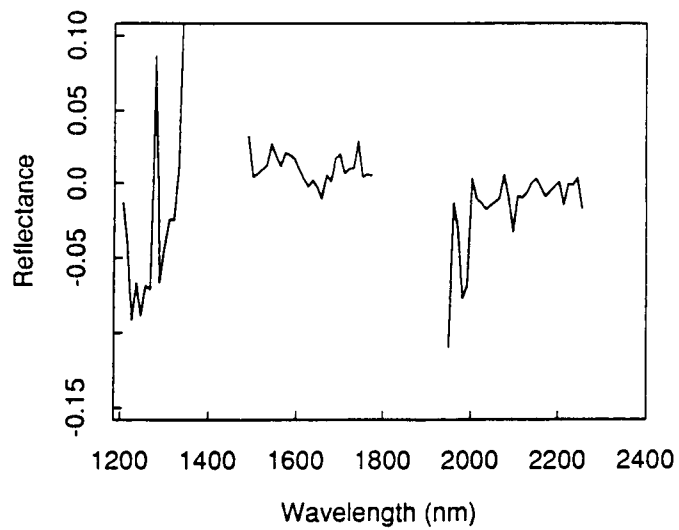Figure 3. System gains (G_b) obtained by solving Equation 1.

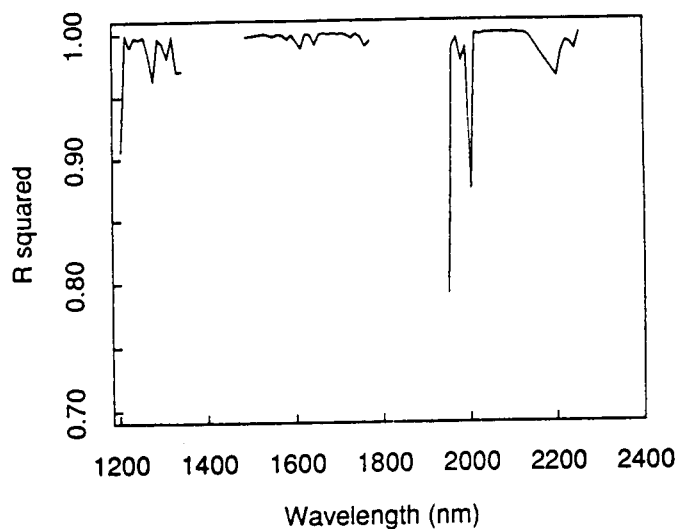Figure 4. System offsets (O_b) obtained by solving Equation 1.

Figure 5. The fit (correlation) between each of the four image and reference endmembers for each band is computed independently.
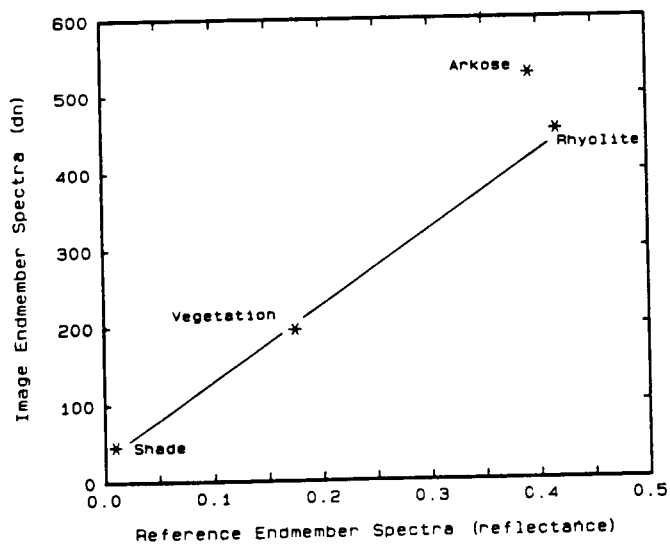

Figure 6. The departure of the reference arkose spectrum from that of the unmixed image arkose endmember spectrum is inferred from the deviation of the arkose endmember from a linear calibration from the other endmembers.

absorption feature can be accomplished by spectrally unmixing the background continium spectrum from that of the arkose (Shipman and Adams 1987).

In summary, we have found that the Tucson AIS-2 image is consistent with each of our initial hypotheses; 1) that the AIS-2 instrument calibration is nearly linear, 2)the spectral variance is caused primarily by sub-pixel mixtures of spectrally distinct materials and shade, and 3) that sub-pixel mixtures can be treated as linear mixtures of pure endmembers. In addition, we have found that the image can be characterized by relatively few spectral endmembers using the AIS-2 high resolution spectra. The resulting patterns in fractions, gains, offsets, and overall fit of Equation 1 to the data make possible the separation of surface effects from those of the instrument, atmosphere, and solar spectrum.

REFERENCES

Adams, J. B., M. O. Smith and P. E. Johnson. 1986. Spectral mixture modeling: A new analysis of rock and soil types at the Viking Lander I Site, J. Geophys. Res. 91, 8098-8112.

Shipman H. M., and J. B. Adams, Detectability of mineral on desert alluvial fans using reflectance spectra, J. Geophys. Res., in press 1987.